

## Atmospheric Spectral Transparency Analysis with Account of the Chemical Atmospheric Composition of the Friction Layer

*D. N. Mishev, V. Jepa-Petrova, I. Lanzov*

Observations on direct solar radiation within the visible and the near infra-red ranges make it possible to obtain series of quantities which characterize the atmospheric transparency in given spectral zones. The juxtaposition of the actual atmospheric response with the ideal optic atmospheric properties (pure and dry atmosphere) together with the chemical analysis of the air in the friction layer could result in some conclusion on the atmospheric aerosol component [1,2].

Taking all that into consideration, the direct solar radiation was observed and the aerosols of the friction layer were chemically analysed on October 23, 1977 at the reference area (Belozem) of the Plovdiv research field with "Radiometer Metrologie" 60-530, equipped with Karl-Zeiss Jena filters. The filters are consistent with the spectral intervals within which the payload is operating.

Table 1 shows the main specifics of the filters we used. As the spectrum of the direct solar radiation is taken at separate discrete points, it is assumed that the solar radiation varies within a linear regularity between two adjacent points.

In the most generalized case, the total solar energy flux, falling to the earth surface  $I_0(\lambda)$  can be represented as a sum

$$(1) \quad I_0(\lambda) = I(\lambda) + I_{OR}(\lambda) + I_{OM}(\lambda),$$

where  $I(\lambda)$  is the flux intensity attenuated by the atmospheric layer,  $I_{OR}(\lambda)$ ,  $I_{OM}(\lambda)$  are the intensities of the Reileigh scattered and Mie scattered radiations, respectively.

Upon direct solar radiation observations we assume that the extinction of the solar radiation when passing through the atmosphere follows Bouguer's law, which is valid for a given meteorological situation: clear and stable weather with visibility distance —  $S_0 > 20$  km, i. e.

$$(2) \quad I_0(\lambda) = S(\lambda) \cdot e^{-\tau m} = S(\lambda) \cdot P^m(\lambda),$$

where  $S(\lambda)$  is the solar spectral irradiance curve,  $P(\lambda)$  is the transparency spectral function,  $m(z)$  is the atmospheric mass and  $\tau$  is the optical atmos-

Table 1

Principal Data on the Filters Used in Ground-Based Observations of Direct Solar Radiation

No. of the filter	$\lambda_{\text{map}}$ (nm)	$\Delta \lambda$ (nm)	$\tau$ %	Sensor permeability coefficient $k(\lambda)$
1	461	7.5	21	0.99
2	480	5.0	24	1.01
3	492	6.5	14	1.03
4	500	5.0	18	1.02
5	523	5.5	37	1.035
6	538	4.0	22	1.036
7	550	4.5	18	1.04
8	574	7.5	40	1.03
9	597	8.0	44	1.015
10	602	6.0	11	1.01
11	619	5.5	18	1.0
12	628	8.0	15	0.98
13	648	7.5	32	0.97
14	659	8.5	22	0.98
15	672	7.0	23	1.01
16	680	7.5	44	1.06
17	708	8.5	26	1.11
18	729	4.5	10	1.1
19	768	10	21	1.02
20	791	8	21	1.08
21	800	7.0	20	1.06
22	894	12	30	1.04
23	930	11	24	1.07
24	975	9.0	20	1.0
25	1055	15	17	0.83

spheric thickness. Those were the conditions on Oct. 23, 1977 at the reference area of Belozem.

We assume that the transparency function can be represented as a product of different multiplicands characterizing the transparency function of the different atmospheric substances. Such assumption could be true if the whole atmosphere were considered to be composed of  $l$  layers, taking into account the amount of attenuated components, and the variation of their optical properties with the height [1].

Accordingly, expression (2) can be represented as

$$(3) \quad I_0(\lambda) = S(\lambda) \prod_{i=1}^l P_i(\lambda, m),$$

where  $l$  is the number of atmospheric layers with determined optical properties.

Within the considered spectral range (460-1,060 nm) such basic components could be ozone, water vapours, aerosol particles. As a result expression (3) will become

$$(4) \quad I_0(\lambda, m) = S(\lambda) \cdot P_{\text{O}_3}(\lambda, m) \cdot P_{\text{H}_2\text{O}}(\lambda, m) \cdot P_{\text{M}}(\lambda, m) \cdot P_{\text{a}}(\lambda, m).$$

Figure 1 shows the standard curve of spectral irradiance  $S(\lambda)$  from [3], the spectral sequence of the solar radiation to the Earth surface in case of Rayleigh scattering and the variation range of the recorded direct solar radiation to the Earth surface  $\Delta I_0(\lambda) = I_{0,\text{max}}(\lambda) - I_{0,\text{min}}(\lambda)$  for Oct. 23, 1977 from 10: 24 h to 14: 50 h. Figure 1 shows that the Rayleigh scatter contributes

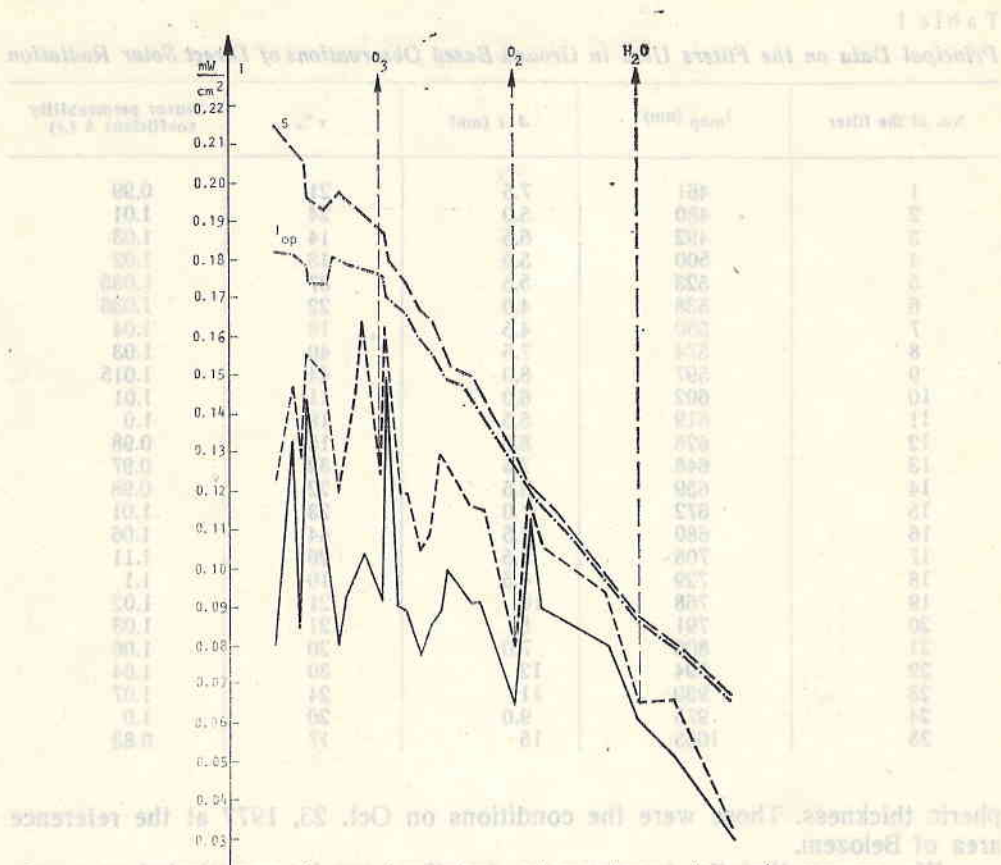


Fig. 1. Solar radiation spectral run;  $S(\lambda)$  standard curve of spectral irradiance;  $I_{op}(\lambda)$  spectral curve in case of Rayleigh scatter.  $I_{0min}$ ,  $I_{0max}$  — minimal and maximal values of the recorded solar radiation on Oct. 23, 1977

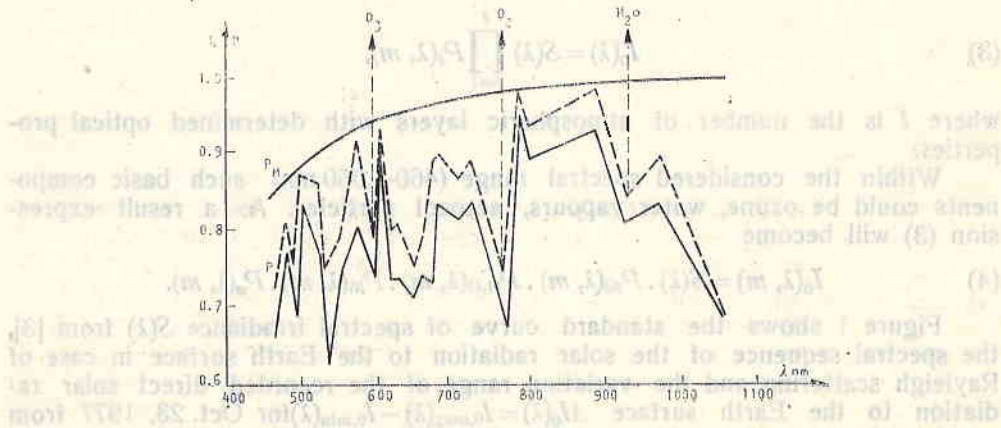


Fig. 2. Transparency spectral curves

Table 2

Composition of Some Elements in Aerosols of the Friction Layer ( $\mu\text{g}/\text{m}^3$ ), Measured at Belozem, Plovdiv District, in November 1977

Cl <sup>-</sup>	SO <sub>4</sub> <sup>2-</sup>	NO <sub>3</sub>
6.04	1.97	2.5
4.85	3.38	2.4
6.40	2.23	2.0
4.40	4.63	2.8

Table 3

Results from Neutron-Activation Analysis of the Content of Some Microelements in the Atmospheric Friction Layer

No.	Litres air	Element	$\mu\text{g}$	$\mu\text{g}/\text{m}^{-3}$	%
1	4430	Al	14	$3.16 \times 10^{-3}$	17.85
2	4430	Fe	10	$2.26 \times 10^{-3}$	12.76
3	4430	Cu	3	$6.80 \times 10^{-4}$	3.84
4	4430	Mn	28	$6.32 \times 10^{-3}$	35.70
5	4430	Na	14	$3.16 \times 10^{-3}$	17.85
6	4430	Co	15	$3.40 \times 10^{-4}$	1.90
7	4430	Mg	$\approx 0.1$	$\approx 2.00 \times 10^{-5}$	0.11
8	4430	Ti	7.5	$1.69 \times 10^{-3}$	9.5
9	4430	Sm	0.09	$2.00 \times 10^{-5}$	0.11
10	4430	Su	0.09	$2.00 \times 10^{-5}$	0.11
11	4430	Rb	$\approx 0.1$	$2.00 \times 10^{-5}$	0.11
12	4430	Ce	$\approx 0.1$	$2.00 \times 10^{-5}$	0.11

significantly to the solar radiative attenuation within the spectral interval of 460-600 nm.

Figure 2 shows the transparency spectral curves of clear, molecular atmosphere  $D_M$  and the transparency variation range of the actual atmosphere.

The lines of oxygen absorption (684-694 nm), (729-770 nm) of the water vapours (700-740 nm), (790-840 nm) and (926-978 nm) are clearly plotted in Figs. 1 and 2. The same can be seen for the wide absorption line of O<sub>3</sub> with maximum of 600 nm. These results agree well with the results of [1]. The simultaneous spectral studies and the chemical analysis of the atmospheric aerosols provide description of the aerosol absorption lines in the visible spectrum.

The concentration of chlorides, nitrides, sulphates, organic and inorganic matter were derived from the aerosol chemical analysis of the friction layer. It was determined that the organic portion represents 27.77% of the dry aerosol, while the inorganic was 72.23%. The presence of organic matter in the friction layer defines the aerosol absorption in the visible range (Fig. 1). Tables 2 and 3 present the results from the chemical aerosol analysis of the friction layer. They show that the concentration of iron in the air is 12.8%, which represents the fourth place with respect to the other elements after

Mn, Na and Al. The high concentration of Fe determines the high absorption capacity of the aerosols within the visible range from 0.46 to 0.68  $\mu\text{m}$ , which is due mainly to the hematite and limonite in the air. This supports also the results obtained in [1]. Another portion of the absorbed radiation within the visible spectrum might be due to sulphur, to small particles of highly absorbable soot, as well as to organic atmospheric particles, as confirmed by the chemical analysis carried out by laboratory techniques.

The varying range width, characterizing the actual atmospheric transparency changes, results from atmospheric dynamic processes, which change the aerosol composition of the friction layer. Since a considerable portion of the solar radiation extinction is due to atmospheric aerosols, small variations in their composition and quantity would result in significant changes of the atmospheric transparency.

Figure 3 shows the optical thickness variations, depending on the atmospheric mass  $m(z)$ .

(5) 
$$\tau(\lambda, z) = \frac{1}{m(z)} \ln \frac{S(\lambda)}{I_0(\lambda)}$$

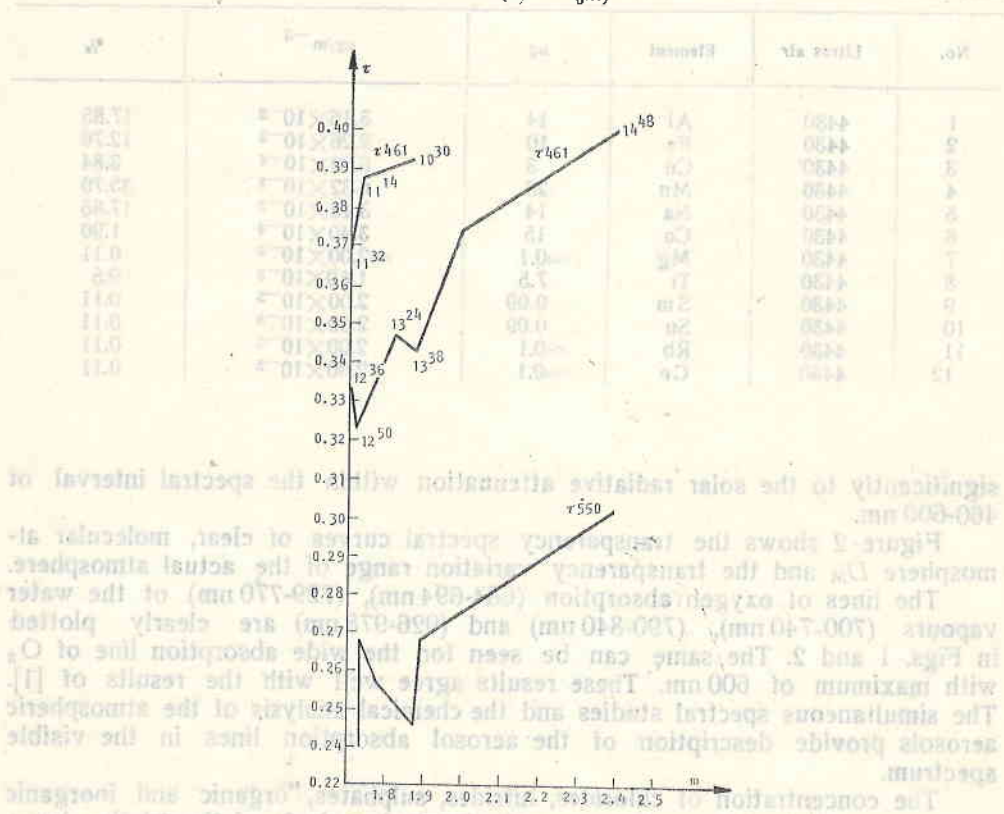


Fig. 3. Optical thickness variation  $\tau$  in dependence on the atmospheric mass on Oct. 23, 1977

Figure 4 shows the atmospheric transparency variations on Oct. 23, 1977 in determined wavelengths during daytime. The transparency increase about noon with the wavelength augmentation is clearly to be seen,

Based on results from determined meteorological conditions and season, it is recommended to photograph the particular research field about noon (12:30 h) when the optical depth is minimal and the transparency is maximal

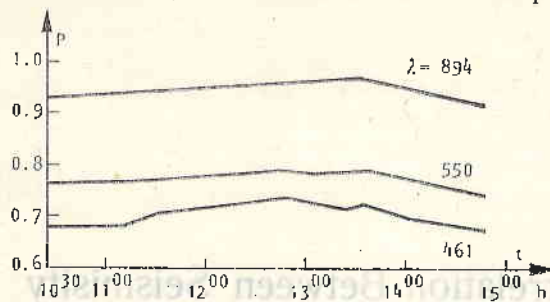


Fig. 4. Atmospheric transparency variation on Oct. 23, 1977

The results obtained show that the chemical analysis of the air in the friction layer which contributes essentially to the solar radiative attenuation, together with the optical observations on direct solar radiation, provide explanation for some spectral intervals of radiative absorption due mainly to the aerosol component in the friction layer.

## References

1. Полный радиационный эксперимент. Под ред. К. Я. Ковдрагеевой, Л., 1966.
2. Twomey, S. Atmospheric Aerosols. New York, 1977.
3. Proceedings of Symposium on Solar Radiations, Nov. 13-15, 1977.

Анализ спектральной прозрачности атмосферы с учетом химического состава атмосферы в приземном воздушном слое

Д. Н. Мишев, В. Джепа-Петрова, И. Ланзов

(Резюме)

В работе показаны результаты экспериментальных исследований спектральной прозрачности атмосферы. Полученные результаты привязаны к химическому составу атмосферы в приземном воздушном слое. Показаны спектральные интервалы поглощения солнечной радиации атмосферными газами и аэрозолем в видимом и ближнем инфракрасном диапазоне.